



Removal of RR198 dye by $\text{TiO}_2/\text{Fe}_3\text{O}_4$ /persulfate nanoparticles under UV-LED irradiation and comparison of OFAT and CCD experimental design in RSM modelling

Somayeh Rahimi¹, Farzaneh Mohammadi*¹ & Zeynab Yavari²

¹Department of environmental health, Firoozabad branch, Islamic Azad University, Firoozabad, Iran

²School of Health, Isfahan University of Medical Sciences, Isfahan, Iran

³Department of Environmental Health Engineering, Abarkouh Parmedical School, Genetic and Environmental Adventures Research Center, Shahid Sadoughi University of Medical Sciences, Yazd, Iran.

E-mail: fm_1363@hlth.mui.ac.ir

Received 25 April 2019; accepted 7 June 2020

The photocatalytic activity of $\text{TiO}_2/\text{Fe}_3\text{O}_4$ nanocomposite has been determined. The XRD spectrum and FESEM analysis have been used to evaluate $\text{TiO}_2 / \text{Fe}_3\text{O}_4$ nanoparticles. The photocatalytic activity of nanoparticles is assessed by degradation of the RR198 solution under the influence of UV-LED radiation. Response Surface Methodology (RSM) is employed to determine the relationships between the studied parameters. The experiments were designed and performed in two ways: One-factor-at-a-time method (OFAT) and Central composite design (CCD). Here nanoparticles with synergistic effect of $\text{S}_2\text{O}_8^{2-}$ were very successful in eliminating the dye. The results of the RSM model with the two mentioned experiment design methods indicated that the model derived from the CCD method had a better predictive capability and favoured from the ability to generalize to other results rather than OFAT method.

Keywords: Nanocomposite, Dye removal, RR198 dye, Photocatalyst, RSM, $\text{TiO}_2/\text{Fe}_3\text{O}_4$

The textile industry is one of the widest industries in the world, whose wastewater has increased in accordance with increasing world demand for the products of this industry and the growth of related industries¹. Discharging of wastewater containing dyes even in low concentration to the receiving water is destructive to the environment due to reduced light penetration and interference in aquatic ecosystems and reducing the photosynthesis of plants and algae^{2,3}. In addition, some of these dyestuffs and products derived from their decomposition are aromatic compounds that are highly carcinogenic and resistant to biological degradation. Finding an effective process for the treatment of wastewater containing these pollutants has resulted in important research efforts⁴. Various methods including adsorption processes, oxidation-reduction, ozonation, biological methods, coagulation and flocculation, and membrane methods have been used to treat wastewater containing dyes. Each of these methods has advantages and disadvantages, the main disadvantage of most of these processes is the addition of secondary pollutants to the environment⁵.

Among above-mentioned treatment methods, photo-oxidation is well acknowledged as a cost-

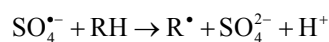
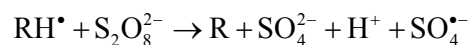
effective alternative. Considering the advantages of photocatalytic degradation like rapid oxidation, lack of polycyclic product formation, oxidation of pollutants at low concentrations, and finally the production of neutral and harmless products, this process has become one of the most promising wastewater treatment methods in comparison with conventional techniques. The hydroxyl radical produced in these processes is a powerful oxidizing agent and completely oxidizes organic pollutants. It is possible that some metal oxides and sulfides were employed as a catalyst for these processes. Produced hydroxyl radicals possess extremely high oxidation power and very low selectivity. Therefore, by producing hydroxyl radicals in treatment processes, a wide range of toxic organic substances, even non-degradable organic substances, is converted into harmless materials such as carbon dioxide and water. The importance of the mentioned process is the nearly complete elimination of pollutants and their conversion into low-risk materials under environmental temperature and pressure. This process has the ability to oxidize a wide range of organic pollutants and eliminate inorganic pollutants, heavy

metals, bacteria and viruses from wastewater. The photo-nanocatalyst process, which employs nanoparticles and is performed by the semiconductor photocatalysts, has been gained considerable attention owing to being low-cost, having low toxicity, favoring from relatively high chemical stability of the catalyst, and the possibility of using sunlight as a source of low-cost radiation⁶⁻⁸.

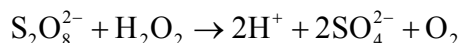
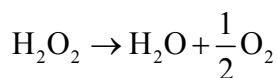
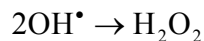
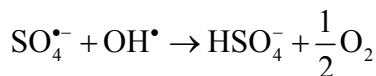
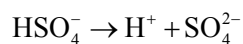
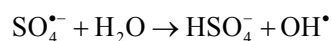
Furthermore, according to the results obtained from the previous studies on the use of UV-LED lamps, there is a need to replace ultraviolet lamps with UV-LED ones due to the superiority of these lamps over ultraviolet lamps and lacking some problems of ultraviolet lamps. These lamps have features such as small size, short response time, low-energy consumption, programming capability for periodic radiation, high vibration and shock resistance and being environmentally friendly⁹. The use of persulfates is proposed as a promising oxidizing agent in the advanced oxidation process due to its high oxidizing properties, non-selective reactivity, high stability and solubility, being economical, as well as the safety and production of active sulfate radicals for the strong and rapid oxidation of pollutants. In these reactions, through the mechanism of electron transfer with the help of intermediate metals, the oxidizing agent can be reduced to produce active radicals that have a high ability to remove organic pollutants¹. If there is a sufficient amount of a bivalent metal cation as an electron donor, for example, the persulfate anion can be converted into sulfate radical according to the following reaction.



Persulfate ion as well as sulfate radical produced through photolysis of the oxidizing agent by light irradiation, according to the following reactions, lead to the breakdown and removal of organic pollutants in an aqueous solution with the production of intermediate radical particles of organic pollutant molecules¹⁰.



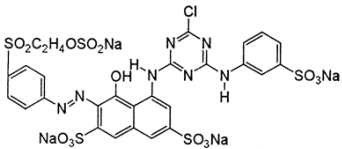
Moreover, the oxidizing agents present in the solution and the relevant intermediates are shown in the following reactions.



The Reactive Red 198 dye with the IUPAC name of tetrasodium;(3~{Z})-5-[[4-chloro-6-(3-sulfonatoanilino)-1,3,5-triazin-2-yl]amino]-4-oxo-3-[[4-(2-sulfonatoxyethylsulfonyl)phenyl]hydrazinylidene]naphthalene-2,7-disulfonate, is red and water-soluble. This is an anionic color and from the chemical point of view belongs to azo dyes¹¹. Table 1 presents the structural formula and properties of the dye:

Given the time-consuming and costly characteristics of laboratory activities and combining modelling with laboratory studies lead to saving time and cost. Designing experiments is one of the most important issues that are being discussed nowadays in various sciences, especially laboratory studies. In fact, statistical design for experiments is a fundamental principle in performing laboratory research. These designs lead to achieving safer results, saving time, and significantly reducing the number of experiments, and ultimately results in process optimization¹². Different modeling techniques such as response surface methodology have the high potential to predict complex processes. Various parameters such as concentration and chemical formula of the pollutant and catalyst, pH, radiation dose and type of radiation, and the amount of energy used in the process as well as the mutual interactions of effective parameters, have a significant effect on the way in which

Table 1 — Reactive Red 198 dye characteristics

Colour Index	C.I.Reactive Red 198
Color Index Number	18221
Azo group	Single azo class
Molecular structure	
Type	Anionic
Molecular Formul	C ₂₇ H ₁₈ ClN ₇ Na ₄ O ₁₆ S ₅
λ _{max} (nm)	518
Molecular weight(g/mol)	968.21

photocatalytic processes operate. The complexity of modeling these processes is having sufficient information on the details of the chemical reactions that occur in the system. To solve these systems, it is needed to write the mass equations and energy equilibrium, whose solving will be very time-consuming and complex. In this situation, the use of mathematical models based on statistical methods such as RSM is very effective and can provide the relationship between all the parameters of the system with linear and nonlinear equations to predict the result¹³. The RSM method is an attractive method for researchers, since they provide a fairly detailed analysis of fewer experiments than conventional factorial methods, and provides a good prediction even for other areas where experiments have not been conducted¹⁴.

In this study, the performance of TiO₂ / Fe₃O₄ nanoparticles align with Persulfate (S₂O₈²⁻) in the removal of RR198 dyestuff in the presence of UV-LED irradiation was studied. Two methods were used to determine the number of experiments. First, by the researchers of this study, the number of experiments was determined with the one-factor-at-a-time (OFAT) optimization method and the results were entered into the RSM model as Historical Data. Then, through the central composite design (CCD) method the number of experiments was also determined, which is much less than the number of experiments in the first method. Next, for both of these two methods, models were developed to predict the amount of pollutant removal rate under the conditions studied by the RSM model and the results were compared with each other.

Experimental Section

The various materials used in this study are titanium dioxide nanoparticles (anatase) from degussa germany, iron (III) chloride, sodium hydroxide, dye Reactive Red 198 and ethanol 99% prepared from Merck Germany, and potassium persulfate (99%) prepared from Sigma-Aldrich Co.

The instruments employed in this study are a digital pH meter (Apera Instruments MP511/ Ohio), a UV-Vis spectrophotometer (SP- 3000 Plus model, Optima, Tokyo, Japan), a magnetic stirrer (Heidolph MR 3001K / Germany), and a scale (Sartorius MSE623P-100-DI) with a precision of ±0.001 and ultrasonic bath (Elma TI-H-5).

Synthesize methodology

To synthesize Fe₃O₄, a solution of FeCl₃.6H₂O and FeCl₂.4H₂O with the concentrations of 1 mol L⁻¹ and

2 mol L⁻¹, respectively, was prepared, poured in a 200-mL beaker, and placed in an ultrasonic bath, then 25 mL of sodium hydroxide (NaOH) of 1 mol L⁻¹ was added to the solution. As the sodium hydroxide solution was added, the black coloured magnetite sediment formed. To complete the reaction, the mixture was placed in a 100-W ultrasonic bath for 40 min (bath temperature of 60°C). The reaction was complete after 40 min. The produced black sediment was separated from the solution by an outer magnetic field (Super Magnet) of 1.32 Tesla and the solvent was spilled out. The sediment was washed several times with deionized water. It should be noted that the above experiments were done in a nitrogen atmosphere.

In the following, for the synthesis of TiO₂ / Fe₃O₄ nanocomposite, 1 g TiO₂ with 1 g Fe₃O₄ in 40 ml of ethanol was placed in the ultrasonic bath for 5 min. The sample was then stirred for 24 hours to evaporate the solvent.

Furthermore, to prepare the dyestuff solution, the stoke solution was prepared at a concentration of 1000 mgL⁻¹ and then other concentrations were prepared by dilution technique.

Investigation of photocatalytic degradation of the synthesized nanocomposite

The photocatalytic activity of the synthesized nanocomposite was studied for the degradation of the RR198 dye, under the irradiation of UV-LED light with a power of 20 W (Fig. 1). Different parameters such as photocatalyst dosage (0.20, 0.40, 0.60, 0.80, and 1.00g/L), initial dye concentration (50, 100, 150, 200, and 250 ppm), persulfate concentration (0.2, 0.4, 0.6, 0.8, and 1 mM) and pH variations (3, 5, 7, 9, and 11) were also evaluated.

The batch system in these experiments was actually a 200-mL beaker, of which 100 mL was filled by the sample and placed on the stirrer. A magnet was thrown into the beaker after cleaning. The sample containing dye pollutants, the oxidizing agent, and the photocatalyst was completely homogeneously stirred in the beaker.

Sampling was carried out at intervals of 0 to 90 minutes, and the absorption rate of dye was determined using spectrophotometer with a wavelength of 518 nm. The efficiency of absorption was obtained using the following equation.

$$\% \text{ dye removal} = \frac{C_0 - C_t}{C_0} \times 100$$

where C₀ and C_t are the dye initial concentration and concentration at each sampling time, respectively.

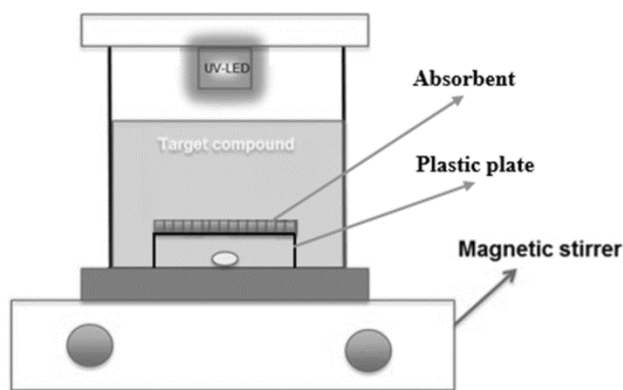


Fig 1 — Schematic UV LED reactor

Data analysis methodology

To determine the effect of the studied parameters on the removal of the RR198 dyestuff via $\text{TiO}_2 / \text{Fe}_3\text{O}_4$ nanocomposite, the RSM model was used in expert design software. The response surface method was applied to find the optimal mode of interaction between factors and to estimate optimal process conditions with the least number of experiments. In this model, the photocatalyst dosage, initial concentration of dye, concentration of persulfate, time and pH variations were introduced to the model as inputs and removal rate of dyestuff was designated as the response parameter. In this study, in order to evaluate the results of the RSM model in the case of a lower number of experiments compared to the more number of experiments two methods were applied: 1- design by using One-factor-at-a-time (OFAT) optimization method and entering the results into the model for analysis through historical data, and 2- the experimental design method of central composite design (CCD).

When the presence of curvature between the levels of the parameters is important, adding more centers to the levels of the factors can lead to a precise determination of the behavior of the function. By adding new centers along the axis of the space between the levels of the factors, the CCD method is achieved. Figure 2 shows the overall design of this method. In this method, each factor is varied in five levels of the lower axis, lower factorial, upper factorial, and upper axis^{15,16}.

In the CCD method, enough information is needed to estimate the lack of fit without excessively increasing the number of experiments. Hence, the number of experiments is obtained by the following equation:

$$L^K + 2K + 1 \quad \dots(1)$$

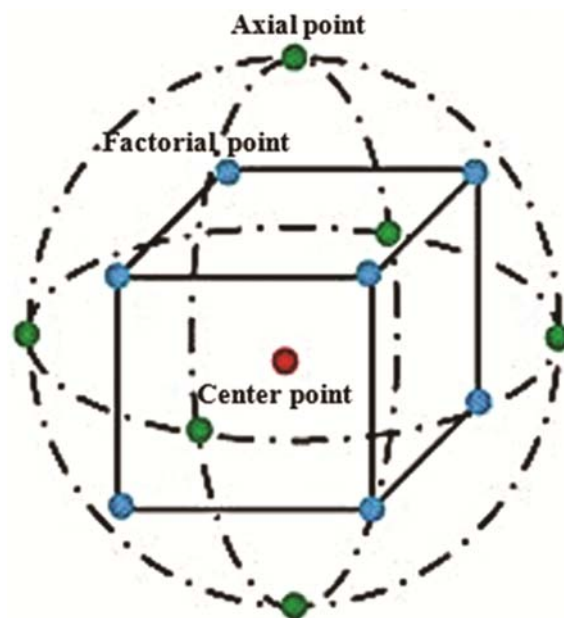


Fig 2 — Experimental strategies for response surface method central composite design (CCD)

where K represents the number of factors investigated in the experiments, and L is the number of levels per factor, and one point is added as the central point to the number of experiments¹⁷.

Another method for designing experiments is the OFAT method. This method, which deals with the optimization of each factor individually, requires more experimenting to obtain a result¹⁸. In this study, the design of the experiments was done in this way too and the results of experiments were introduced into the RSM model in Design Expert software using the historical data method¹⁹.

The results of the experiments entered into both methods were modeled using the RSM model to determine the appropriate equation. The second-order polynomial equation was used to define the relationships between the parameters.

$$y = \beta_0 + \sum_{i=1}^k \beta_i X_i + \sum_{i=1}^k \beta_{ii} X_i^2 + \sum_{i=1}^k \sum_{j=1}^k \beta_{ij} X_i X_j + \varepsilon \quad \dots(2)$$

where y is the predicted responses, $X_{i,j}$ is the encoded independent variables, k represents the number of variables, β_0 is a constant of the model, β_i , β_{ii} , and β_{ij} are respectively the coefficients of linear variables, coefficients of variables with second order, and coefficients of the interactions of the variables, and ε is the error rate. To experiment reliability, one-way analysis of variance (ANOVA) should be performed. In this model, the coefficient of determination (R^2) was used to evaluate the fitness of the model and the F-experiment was employed to check the lack of fit.

In most RSM modelling, it is appropriate for independent variables to be converted to the encoded variables of x₁, x₂, ..., x_n [20]. In this study, the value of independent variables was coded between -2 and +2 [21]. In Tables 2 and 3, the variables and the number of experiments are presented for both of the methods.

Results and Discussion

Figure. 3 demonstrates the XRD pattern of the synthesized nanocomposite in comparison with TiO₂. The position and relative intensity of peaks in the XRD pattern of the TiO₂ / Fe₃O₄ indicate the presence

of crystalline Fe₃O₄ phases in the synthesized photocatalyst structure.

In Fig. 4, the FESEM image of the TiO₂ / Fe₃O₄ particles synthesized through co-precipitation process is shown. These particles have spherical morphology and have a very neat arrangement.

Investigating the effect of different parameters on the process of photocatalytic removal in the OFAT method

Investigating the effect of initial dye concentration

In Fig. 5-A, the removal efficiency is shown in different initial concentrations of RR198 dye in respect to time. These experiments were carried out at

Table 2 — Variables levels applied in RSM through the CCD method

Parameters		level				
		-2	-1	0	+1	+2
A	C ₁ -RR198 (mg/l)	50	100	150	200	250
B	pH	3	5	7	9	11
C	TiO ₂ -Fe ₃ O ₄ (mg/l)	100	200	300	400	500
D	Time (min)	10	30	50	70	90
E	S ₂ O ₈ (mM)	0.2	0.4	0.6	0.8	1
Total number of experiments		50				

Table 3 — Variables levels applied in RSM through OFATmethod

Parameters	Number of levels					Number of experiments
	C ₁ -RR198	pH	TiO ₂ -Fe ₃ O ₄	S ₂ O ₈	Time	
C ₁ -RR198	5	1	1	1	5	25
pH	1	5	1	1	5	25
TiO ₂ -Fe ₃ O ₄	1	1	5	1	5	25
S ₂ O ₈	1	1	1	5	5	25
Total number of experiments		100				

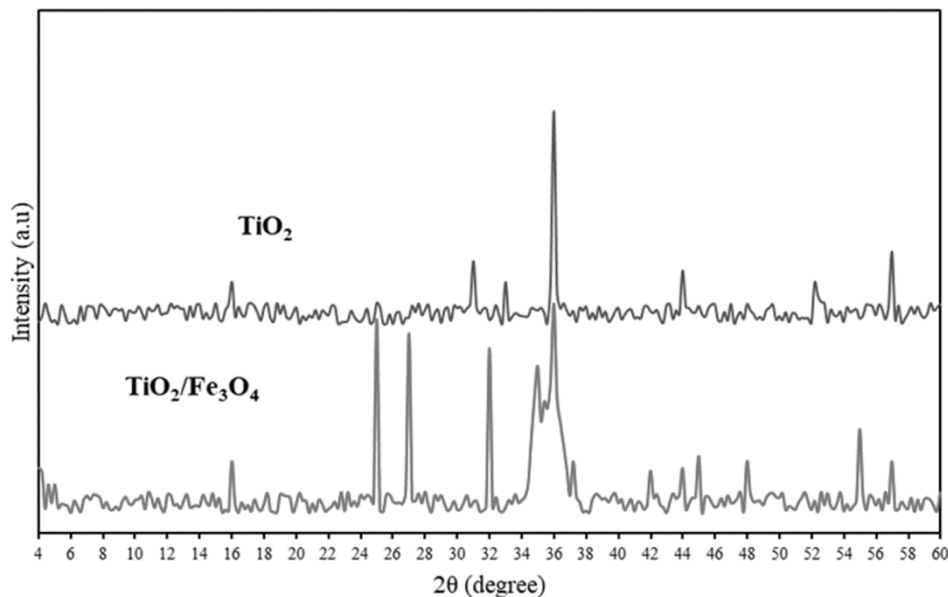


Fig 3 — XRD pattern

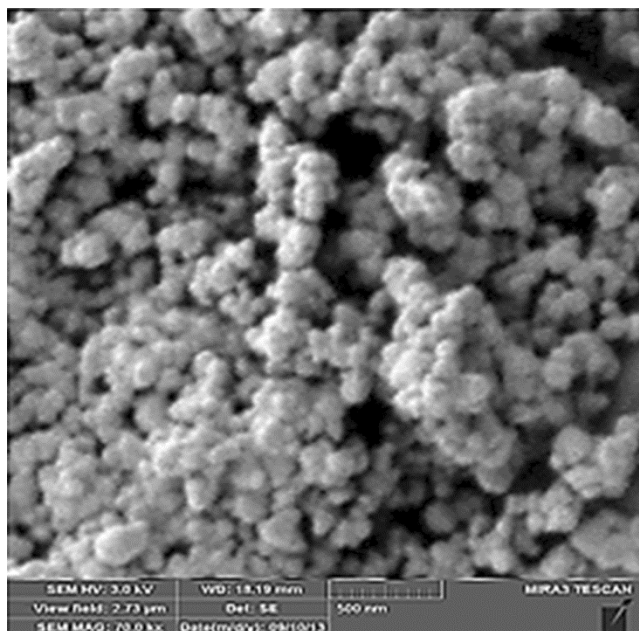


Fig 4 — FESEM images for $\text{TiO}_2 / \text{Fe}_3\text{O}_4$ particles

a constant $p\text{H}$ of 3, a photocatalyst dosage of 500 mg/L, and a persulfate concentration of 1 mM. Based on the plotted graphs, with an increase in dye concentration from 50 mg/l to 250 mg/L, the amount of pollutant removal significantly decreased. Furthermore, the dye removal rate increased over time, until about 90 minutes. It should be noted that after about 70 min, the dye removal at all concentrations was almost stable and the slope of graphs decreased significantly. At high concentrations of dye pollutants, the light penetration into the solution was reduced and the efficiency of the removal process decreased. In fact, increasing the dye concentration in the solution acted as a light filter and reduced the removal. Of course, it is worth mentioning that reduction in the light amount leads to a reduction in the photolysis of $\text{S}_2\text{O}_8^{2-}$ and the production of hydroxyl and sulfate radicals. Moreover, at the same concentration of oxidizing agent ($\text{S}_2\text{O}_8^{2-}$), an increase in the amount of dye pollutant can lead to a reduction in the amount of dye removal due to the limited amount of oxidizing agent in the solution compared to the dye concentration.

Investigating the effect of photocatalyst dosage

In Fig. 5-B, the removal rate in different photocatalyst dosage is demonstrated in respect to time. These experiments were carried out at a constant $p\text{H}$ of 3, an initial RR198 concentration of 250 mg/l

and a persulfate concentration of 1 mM. Based on the plotted graphs, with the increase of the photocatalyst, the active sites available for absorbing the pollutant increased. However, with increasing photocatalyst, UV light was dispersed by particles, and in the low photocatalyst dosage, the amount of absorbing sites available in the environment decreased, and thereby, the degradation rate declined.

Investigating the effect of $p\text{H}$

In Fig. 5-C, the removal efficiency in different values of $p\text{H}$ is displayed in respect to time. These experiments were performed at a photocatalyst dosage of 500 mg/L, an initial RR198 concentration of 250 mg/L and a persulfate concentration of 1 mM. The results showed that the dye removal rate in acidic $p\text{H}$ was significant. The effect of $p\text{H}$ on the photocatalytic removal of the pollutant is related to the electrostatic forces governing the surface of the metal oxide and the pollutant. Due to the anionic nature of the dye, the electrostatic attraction forces happened between the photocatalyst and the dyestuff in acidic $p\text{H}$. Thus, in basic environments, the removal rate will be lower.

Investigating the effect of persulfate concentration

In order to investigate the effect of potassium persulfate concentration on the dye removal rate, an experiment, in which the initial RR198 concentration, photocatalyst dosage, and constant $p\text{H}$ were respectively 250 mg/L, 500 mg/L, and 3, was designed to investigate the removal at certain concentrations of $\text{S}_2\text{O}_8^{2-}$. The obtained results, demonstrated in Fig. 5-D, indicates that with increasing $\text{S}_2\text{O}_8^{2-}$ concentration, the removal rate increased from 0.2 mM to 1 mM. This increase is justified in that increasing the production of hydroxyl and sulfate radicals owing to increased persulfate concentration.

Kaurb and Singh studied the degradation of Reactive Red 198 by TiO_2 mediated photocatalytic align with UV irradiation. The initial dye concentration (50 to 200 mg/l), photocatalyst dosage (50 to 500 mg/L) and $p\text{H}$ (3 to 11) were investigated and the results have a good agreement with the results of this research²².

Sohrabi et al. examined the removal of DR23 by several photocatalyst (UV / TiO_2 , UV / SnO_2 , UV / Fe_2O_3 , UV / ZnO). The best photocatalyst was recognized to be the UV- TiO_2 . $p\text{H}$ ranged from 2 to 9 and the best $p\text{H}$ was selected to be 2. The study time

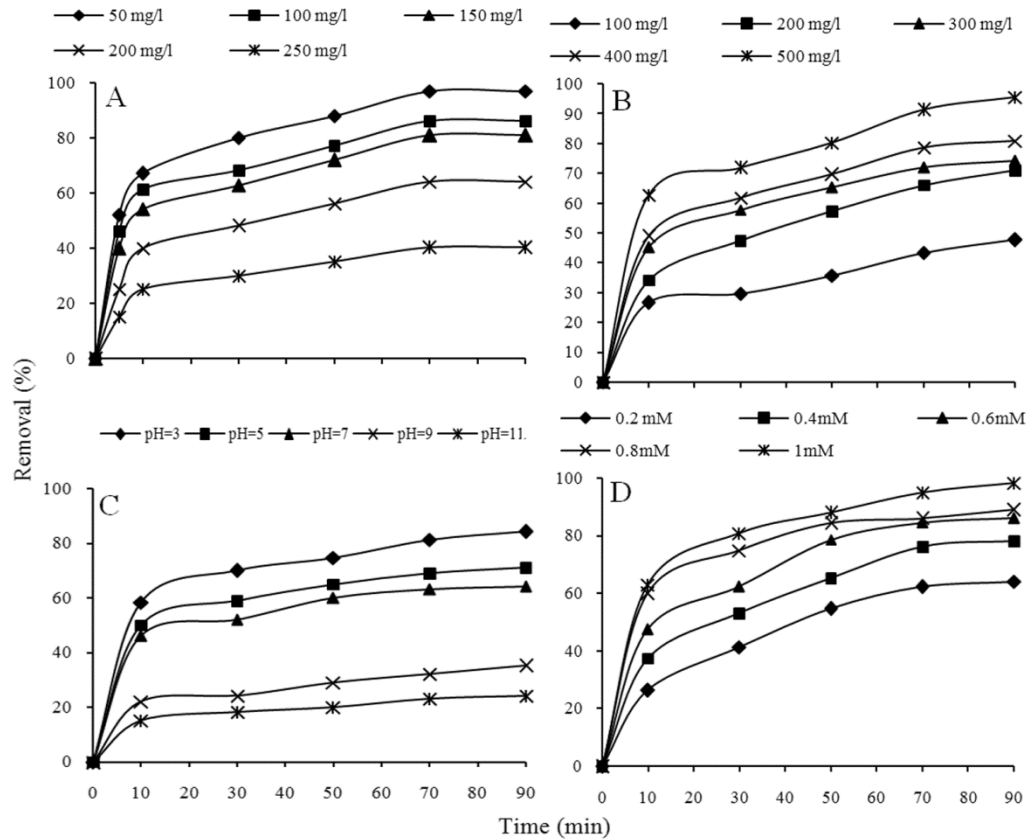


Fig 5 — Investigation the effect of A- initial dye concentration B- photocatalyst dosage C- pH D- persulfate concentration

was evaluated from 0 to 90 minutes. At all concentrations studied, an increase in removal rate was seen up to 60 minutes after the start of the reaction, and then no significant change was observed in the removal rate²³.

Investigating the results of RSM model in the design of experiments by OFAT and CCD methods

The statistical design of the experiments was performed using CCD and OFAT methods to determine the effect of the considered independent parameters on RR198 removal. The nonlinear quadratic equations were driven from the results obtained from two methods, which are presented below. The equations are provided after the elimination of terms whose p-value was more than 0.05 and were not significant.

The equation obtained from the CCD Design experiments:

$$\begin{aligned}
 \text{Removal rate} = & 56.61 - 4.93A - 18.33B + 4.42C \\
 & + 6.88D + 4.49E + 3.0AB \\
 & + 2.71AC - 2.14AD - 2.72BC \\
 & - 3.13BD - 2.77B^2 - 3.75C^2 \\
 & - 3.57D^2 - 2.46E^2
 \end{aligned}$$

Table 4 — ANOVA analysis for the selected quadratic model					
Source	F-Value	P-Value	Result	R-Squared	Adjusted R-Squared
CCD					
model	27.29	< 0.0001	Significant	0.9161	0.8925
Lack of Fit	3.14	0.0607	Not significant		-
OFAT					
model	162.66	< 0.0001	Significant	0.9523	0.9464
Lack of Fit	1.24	0.3086	Not significant		-

The equation obtained from the OFAT Design experiments:

$$\begin{aligned}
 \text{Removal rate} = & 19.84 - 18.11A - 26.64B \\
 & + 18.33C + 11.62D + 15.30E \\
 & - 3.90AD - 7.48BD - 2.45DE \\
 & - 2.80A^2 - 3.94B^2 - 15.60C^2 \\
 & - 4.19D^2 - 6.12E^2
 \end{aligned}$$

As previously mentioned, in the above equations, A, B, C, D and E were the initial dye concentration, pH, TiO₂-Fe₃O₄ dosage, time, and S₂O₈²⁻ concentration, respectively.

Also, the results of one-way ANOVA used for both the proposed model are presented in Table 4.

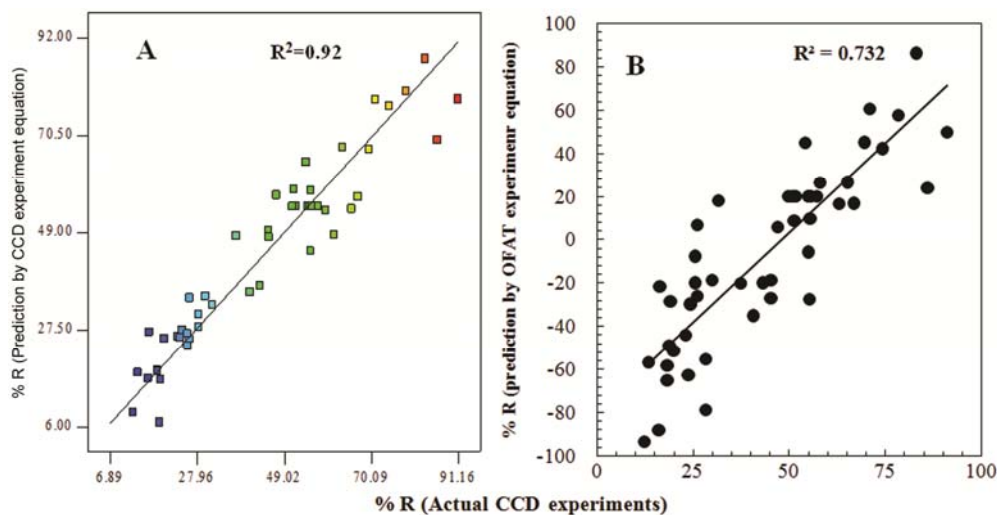


Fig 6 — Prediction of the CCD experiments by the proposed RSM model A-CCD B-OFAT

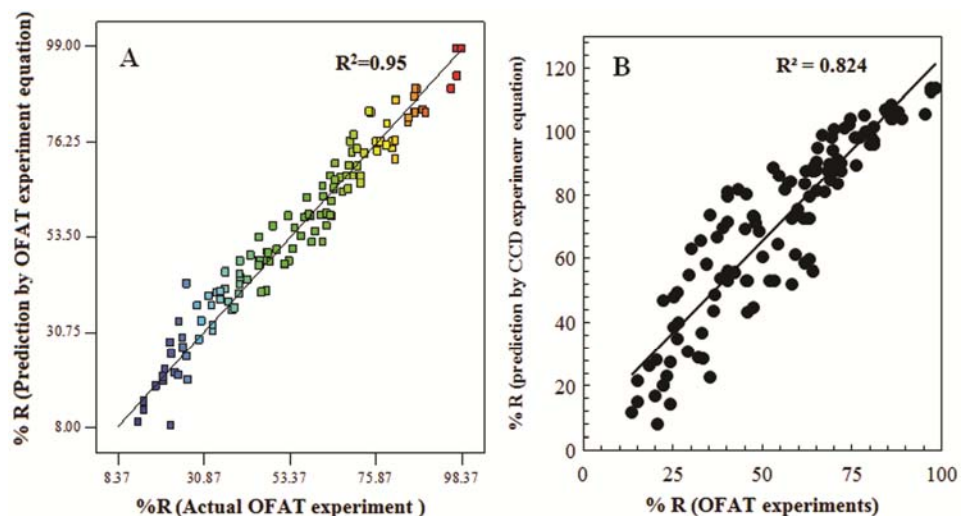


Fig 7 — Prediction of the OFAT experiments by the proposed RSM model A-OFAT B-CCD

The Fisher test was employed to examine the significance of the model. In the main model, the p-value should be less than 0.05 so that the model would be significant at a confidence level of 95% and for the lack of fit, the p-value should be greater than 0.05 in order that errors are not significant. In both methods, experiments have achieved acceptable results. The determination coefficient (R^2) values indicate that although both experimental design methods have been a good predictor of the available results, the OFAT method has been found to have a higher R^2 for predicting the results of related experiments (Figs. 6-A and 7-A).

To evaluate the performance of the equation provided in each method and the accuracy of its results for other methods, the results of the OFAT experiments were predicted by the model

proposed in the CCD method (Fig. 7-B) and also the model proposed in the OFAT method was used to predict the results of the CCD experiments (Fig. 6-B).

As shown in Fig. 7-B, the equation obtained from the experiments conducted through the CCD method has appropriately been able to predict the OFAT experiment with $R^2 = 0.82$. The average of the results of the actual experiments by the OFAT method was about 55%, while the equation obtained by the CCD method predicted the average about 64%.

But according to Fig. 6-B, the equation obtained by the OFAT method has not been able to predict the results of experiments by the CCD method at all. Although the predicted value of $R^2 = 0.73$ does not seem to be very inappropriate, the average of the results of the actual experiments by the CCD method was about 44%,

while the equation obtained by the OFAT method predicted for an average of -6.5%, indicating a significant difference with actual values. Although the number of experiments in the CCD method (50) is even less than half the number of experiments in OFAT (130), it seems that the model derived from the CCD method has a much higher reliability, which can be due to the appropriate distribution of design experiments in the first step of the study.

Alshehria *et al.* concluded a study in 2016 and found that the optimization of a variable by the OFAT method and holding the other variables levels constant

could not show the interactions between variables. They mentioned that this method was very time-consuming and required more experimenting to determine the optimal point of the system. All the disadvantages of this method can be resolved using statistical methods of designing experiments such as CCD²⁴.

In order to examine the results of the RSM model in the design of experiments by OFAT and CCD methods, the graphs of Fig. 8 were depicted. As can be seen, although the number of experiments in the CCD method is much less than the OFAT method,

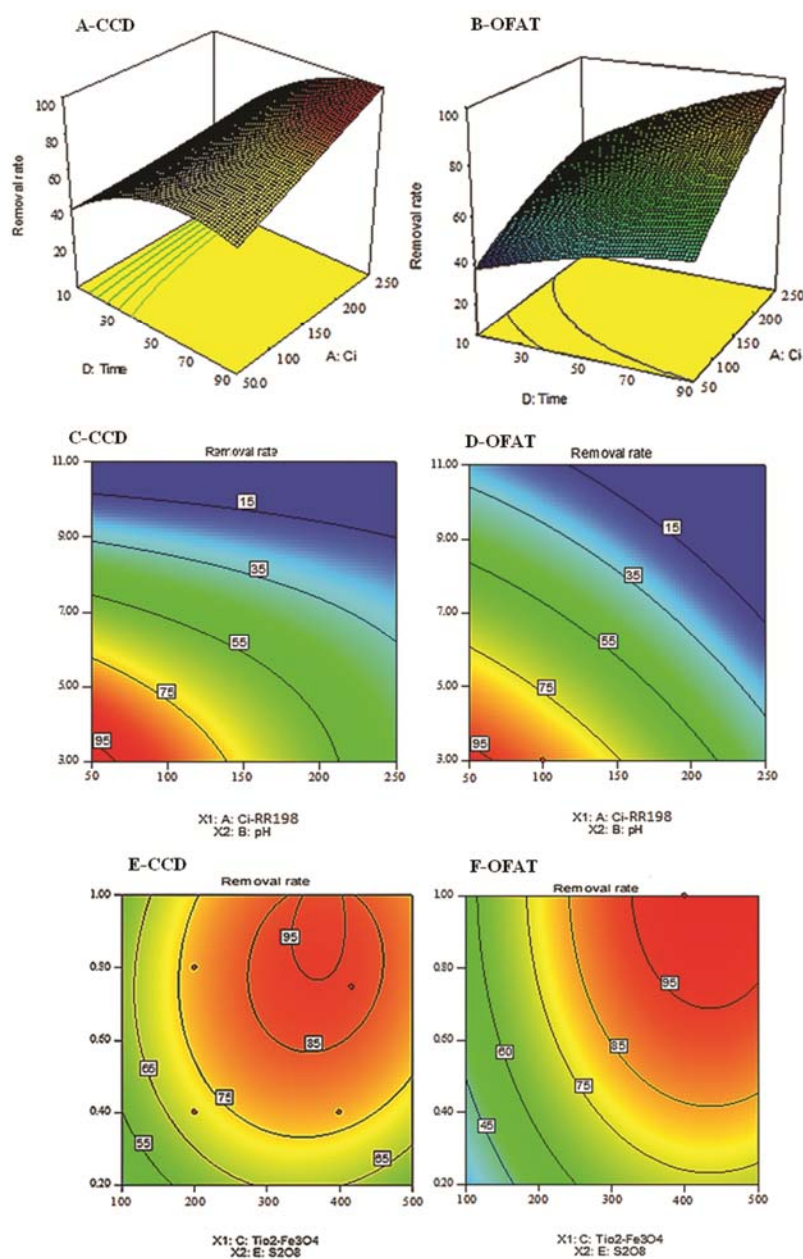


Fig 8 — RSM model outputs

the diagrams trends of initial dye concentration, pH, $\text{TiO}_2/\text{Fe}_3\text{O}_4$ dosage, and $\text{S}_2\text{O}_8^{2-}$ concentration are roughly the same. Based on Fig. 8-A and 8-B, in both methods, the removal rate has been reduced by increasing the initial dye concentration and, with increasing reaction time, the removal rate has been improved. In both graphs, at the pH of 3, the $\text{S}_2\text{O}_8^{2-}$ concentration of 1 ppm, and $\text{TiO}_2/\text{Fe}_3\text{O}_4$ dosage of 500 mg/l, the removal rate at various initial dye concentrations is estimated to range from 40 to 100%. According to Figs 8-C and 8-D, the best pH was about 3 in both methods and at pH more than 7 and dye concentrations higher than 200 mg/l, efficiency was never exceeded than 55%. Figs. 8-E and 8-F show that, in both methods, the best concentration of $\text{S}_2\text{O}_8^{2-}$ is 0.8 ppm to 1 ppm and best dosage of $\text{TiO}_2/\text{Fe}_3\text{O}_4$ is 400 mg/l for initial dye concentration about 50 mg/L.

Investigation of changes in the absorption spectrum before and after the removal of the RR198

Figure. 9 shows the absorption spectrum of the RR198 in a range of 200 to 700 nm at different time intervals from the beginning of the oxidative degradation reaction. The absorption spectrum of the RR198 has 2 maximum peaks at wavelengths about 500 to 510 nm and 290 to 300 nm. According to the Fig. 9, it is observed that with the advancement of the reaction, the intensity of the peaks in the dye absorption spectrum decreases and the absorption rate in these absorption peaks decreases to zero, indicating the process of degradation and removal of dye molecules.

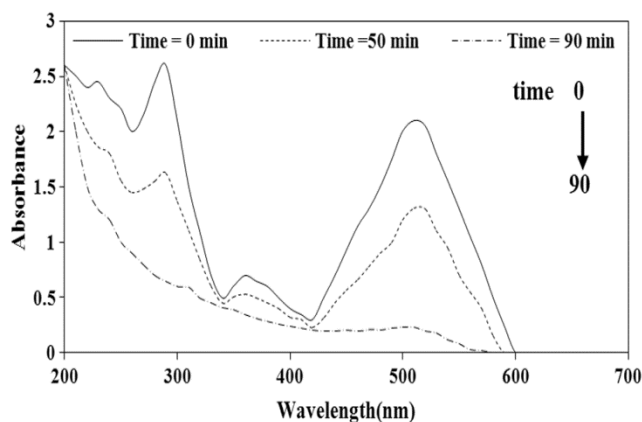


Figure 9 — Trends of changes in the absorption spectrum in the removal of the RR198

$\text{TiO}_2/\text{Fe}_3\text{O}_4=500$ mg/L, $[\text{S}_2\text{O}_8^{2-}] = 1\text{mM}$, $[\text{RR198}] = 50$ mg/L, $\text{pH} = 3$

Conclusion

In this study, the removal of Reactive Red 198 dyestuff from aqueous solutions using $\text{TiO}_2 / \text{Fe}_3\text{O}_4$ nanoparticles under the irradiation of UV-LED has been examined. The initial dye concentration in the range of 50 to 250 mg/L is investigated. Determining the optimal point of the process's performance is very effective in achieving the desired results. The results of this study show that the best pH for RR198 removal is acidic pH equivalent to 3. The dye is maximally eliminated after about 70 min from the start of the experiment. The best concentration of $\text{TiO}_2 / \text{Fe}_3\text{O}_4$ and $\text{S}_2\text{O}_8^{2-}$ nanoparticles is found to be 400 mg/L and 1 mM, respectively in low initial dye concentration. Presence of potassium persulfate increased the removal efficiency. Response Surface Methodology (RSM) was applied to determine the relationships between the studied parameters and to optimize of the results. The experiments were designed and performed in two ways: One-factor-at-a-time method (OFAT) and Central composite design (CCD). In both methods, the nonlinear second-order RSM model is in good agreement with the experimental results so that the coefficient of R^2 between the experimental results and the prediction of the models obtained from CCD and OFAT was 0.92 and 0.95, respectively. The model derived from the CCD method also show good ability to predict the results of the OFAT method while the model derived from experiments designed by the OFAT method did not show any good performance in predicting the results of the CCD method. The results of the RSM model with the two mentioned design of experiments indicate that although the number of experiments in the CCD method is even less than half the number of experiments in the OFAT method, the CCD model had better predictive capability and ability to generalize to other results, which can be due to the appropriate distribution of experiments designed in the first step of the study.

Acknowledgement

This article is the result of researches approved in the Isfahan University of Medical Sciences (IUMS). The authors wish to acknowledge to Vice Chancellery of Research of IUMS for the financial support, Research Project, # 198141 and ethics code IR.MUI.RESEARCH.REC.1398.489

References

- 1 Gemeay A H, Habib A F M & Borhan El-Din M A, *Dye Pigment*, 74 (2007) 458.
- 2 He H Y, J Huang F, Cao L Y & Wu J P, *Desalin*, 252 (2010) 66.
- 3 Konstantinou I K & Albanis T A, *Appl Catal B Environ*, 49 (2004) 1.

- 4 Mittal H, Alhassan S M & Ray S S, *J Environ Chem Eng*, 6 (2018) 71190.
- 5 Katheresan V, Kansedo J & Lau S Y, *J Environ Chem Eng*, 6 (2018) 4676.
- 6 Horikoshi S & Serpone N, *Catal Today*, (2018) 81.
- 7 Zhao D & Wu X, *Mater Lett*, 210 (2018) 354.
- 8 Yahya N, Aziz F, Jamaludin N A, Mutalib M A, Ismail A F, Salleh W N W, Jaafar J, Yusof N & Ludin N A, *J Environ Chem Eng*, 6 (2018) 7411.
- 9 Hu X, Li G & Yu J C, *Langmuir*, 26 (2010) 3031.
- 10 Ranga Rao A & Dutta V, *Sol Energy Mater Sol Cells*, 91 (2007) 1075.
- 11 Lucilha A C, Bonancêa C E, Barreto W J & Takashima K, *Spectrochim Acta Part A Mol Biomol Spectrosc*, 75 (2010) 389.
- 12 Saldaña-Robles A, Guerra-Sánchez R, Maldonado-Rubio M I & Peralta-Hernández J M, *J Ind Eng Chem*, 20 (2014) 848.
- 13 Bolanča T, Ukić Š, Peternel I, Kušić H & Lončarić Božić A, *Indian J Chem Technol*, 21 (2014) 21.
- 14 Gasemloo S, Khosravi M, Sohrabi M R, Dastmalchi S & Gharbani P, *J Clean Prod* 208 (2019) 736.
- 15 Aslan N & Cebeci Y, *Fuel*, 86 (2007) 90.
- 16 Montgomery D C, *Design Analysis of experimentsat*
- 17 ArsalaniN, Nasiri R & Zarei M, *Chem Eng Res Des*, 136 (2018) 795.
- 18 Simonoska Crcarevska M, Geskovski N, Calis S, Dimchevska S, Kuzmanovska S, Petruševski G, Kajdžanoska M, Ugarkovic S & Goracinova K, *Eur J Pharm Sci*, 49 (2013) 65.
- 19 Gagliardi F, Ambrogio G, Ciancio C & Filice L, *J Manuf Syst*, 45 (2017) 195.
- 20 Gadekar M R & Ahammed M M, *J Environ Manage*, 231 (2019) 241.
- 21 Singh N & Balomajumder C, *J Water Process Eng*, 11 (2016) 130.
- 22 Kaur S & Singh V, *J Hazard Mater*, 141 (2007) 230.
- 23 Sohrabi M R & Ghavami M, *J Hazard Mater*, 153 (2008) 1235.
- 24 Alshehria A N Z, Ghanem K M & Al-Garni S M, *J Taibah Univ Sci*, 10 (2016) 797.